

Mesostructured materials for optical applications: from low-k dielectrics to sensors and lasers[☆]

Gernot Wirnsberger^{a,*}, Peidong Yang^b, Brian J. Scott^c,
Bradley F. Chmelka^d, Galen D. Stucky^{c,1}

^a Department of Chemistry, Inorganic Chemistry Karl-Franzens-University Graz 8010 Graz, Austria

^b Department of Chemistry, University of California, Berkeley, CA 94720, USA

^c Department of Chemistry and Biochemistry, University of California, Santa Barbara, CA 93106, USA

^d Department of Chemical Engineering, University of California, Santa Barbara, CA 93106, USA

Received 15 October 2000; accepted 04 December 2000

Abstract

Recent advances on the use of mesoporous and mesostructured materials for electronic and optical applications are reported. The focus is on materials which are processed by block-copolymer templating of silica under weakly acidic conditions and by employing dip- and spin-coating as well as soft lithographic methods to bring them into a well-defined macroscopic shape. Several chemical strategies allow the mesostructure architecture to be used for electronic/optical applications: Removal of the block-copolymers results in highly porous, mechanically and thermally robust materials which are promising candidates for low dielectric constant materials. Since the pores are easily accessible, these structures are also ideal hosts for optical sensors, when suitable are incorporated during synthesis. For example, a fast response optical pH sensor was implemented on this principle. As-synthesized mesostructured silica/block-copolymer composites, on the other hand, are excellently suited as host systems for laser dyes and photochromic molecules. Laser dyes like rhodamine 6G can be incorporated during synthesis in high concentrations with reduced dimerization. This leads to very-low-threshold laser materials which also show a good photostability of the occluded dye. In the case of photochromic molecules, the inorganic–organic nanoseparation enables a fast switching between the colorless and colored form of a spirooxazine molecule, attributed to a partitioning of the dye between the block-copolymer chains. The spectroscopic properties of these dye-doped nanocomposite materials suggest a silica/block-copolymer/dye co-assembly process, whereby the block-copolymers help to highly disperse the organic dye molecules. © 2001 Elsevier Science B.V. All rights reserved.

Keywords: Mesoporous materials; Mesostructures; Sol-gel chemistry; Block-copolymer templating; Nanostructures

[☆] Dedicated to Professor Harald P. Fritzer on the occasion of his retirement.

* Corresponding author. Fax: + 43-3842-322564.

E-mail address: gernot.wirnsberger@kfunigraz.ac.at (G. Wirnsberger).

¹ Corresponding co-author. Fax: + 1-805-8934120, stucky@chem.ucsb.edu (G.D. Stucky).

1. Introduction

Mesoporous materials are an interesting class of materials for technological applications due to their regularly arranged 3-dimensional pores. They are synthesized by co-assembly of an inorganic component (e.g. silica) and surfactants [1] or block-copolymers [2,3]. After calcination, the pores are freely accessible which makes these compounds useful for separation, sorption and catalytic applications [4–6]. More recently, mesoporous materials have also attracted interest for electronic and optical applications. It has been recognized that these porous systems with pore sizes between ~ 2 and 20 nm are promising candidates for the next-generation low- k dielectric materials for integrated circuits [7,8]. Also, the highly porous nature of these materials makes them excellent hosts for sensing molecules/ions, since the species to be sensed can easily diffuse towards the sensing center.

As-synthesized mesostructured materials, i.e. materials in which the surfactants/block-copolymers are not removed, have recently been exploited for the low-temperature synthesis of optical materials by using dye-doping [9,10]. For sol-gel glasses, low-temperature dye-doping has been reported nearly two decades ago [11] and ongoing research has led to the introduction of optically active sol-gel glasses into the market. However, all the advantages of sol-gel glasses (high dye dispersion, mechanical robustness, transparency of the matrix in the visible to UV range, high processibility, etc.) are also present in mesostructured materials. Moreover, as we will outline below, simultaneous silica/block-copolymer/dye co-assembly can lead to improved optical characteristics. The key point is the nanoscopic structure built up by the silica and the polyethylene oxide–polypropylene oxide–polyethylene oxide (PEO–PPO–PEO) triblock-copolymers that leads to structurally ordered inorganic/organic arrays with an ordering length scale of about ~ 2 to 20 nm. These nanostructures, a schematic example of which is depicted in Fig. 1, provide different microenvironments available to the dyes incorporated during synthesis. From that viewpoint, a block-copolymer/silica

mesostructure can be regarded as a system containing three chemical ‘sub-phases’: The hydrophobic PPO block, the hydrophilic PEO block, and the silica wall, whereby the PEO block also extends into the silica wall [12]. Of course, the occlusion of a dye into preferentially one or maybe more sub-phases will be determined by chemical interactions like electrostatic forces, hydrogen bonding, and dispersion forces.

In this paper, we describe and discuss the synthesis and characterization as well as the performance and possible applications of low- k dielectric mesoporous materials, mesoporous optical sensors, and optically active mesostructured composites like lasers and photochromic materials. We demonstrate how both the ‘empty’ pores and the surfactant-filled pores can be utilized to construct novel nanostructured materials with useful electronic/optical properties.

2. Experimental

2.1. Materials

Mesostructured silica/block-copolymer composites were prepared from solutions containing (in molar ratios) tetraethylorthosilicate:ethanol:

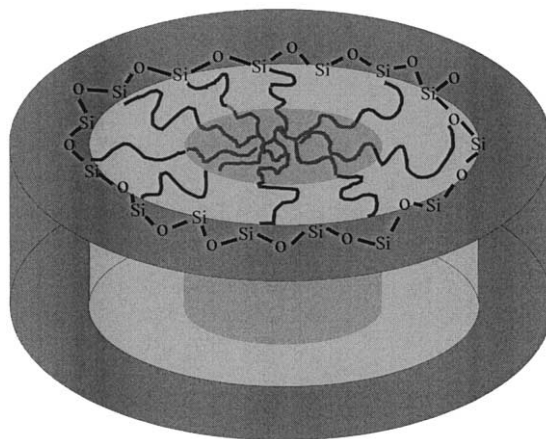


Fig. 1. Schematic illustration of a hexagonal silica/block-copolymer mesostructure showing the polypropylene oxide/polyethylene oxide/silica nanophase separation.

H₂O:HCl:block-copolymer = 1.0:22.15:5.0:0.02:0.008–0.02. Although a variety of different block-copolymers can be employed successfully for mesostructure synthesis [3], we here focus on compounds made by either Pluronic P123 (PEO₂₀PPO₇₀PPO₂₀) or Pluronic F127 (PEO₁₀₇PPO₇₀PEO₁₀₇) [13]. After the reagents had been mixed to give homogenous solutions, the latter were held at temperatures between 60 and 80°C for 1 h. Afterwards, these solutions were processed into thin films by employing dip- or spin-coating [7], into 1–10 μm diameter waveguides by soft lithographic methods [14], or into coatings on optical fibers by dip-coating the latter [15]. If a calcination step (oxidative surfactant removal at elevated temperatures) was necessary, the materials were usually heated to 400°C within 6 h, hold at this temperature for 4 h and were finally cold down within 4 h to room temperature.

2.2. Materials characterization

For dielectric constant measurements, highly-doped Si wafers were used as substrates for the dip-coating deposition process. The as-made films were calcined in air at 500°C for 5 h followed by vapor treatment using hexamethyldisilazane (HMDS) or octadecyltrichlorosilane (OTS). The dielectric constants of the mesoporous silica thin films were calculated from the measured capacitance. For capacitance measurements, the back-side of the wafers were coated with an Al layer. On the top of the films, an array of Al dots, each about 100 nm thick and 1 mm² in area, was deposited using a shadow mask. Capacitance measurements were performed with an HP 4192A LF meter under ambient conditions. The frequency during the measurement was varied from 10 Hz to 13 MHz; most of the measurements were carried out using 1 MHz. Refractive index measurements were carried out by variable angle spectroscopic ellipsometry. Refractive indices were fitted by employing an air/silica model taking the porosity of the films into account. The thickness of the films were measured using a Dektak profilometer or by carrying out cross-section scanning electron microscopy imaging.

All emission measurements were performed on

an optical bench enabling a variable setup. For investigating pH sensing with mesoporous thin films, films were dipped into pH buffer solutions and the front-face emission was measured by exciting the samples with the 488 nm line of an Ar⁺ ion laser. For the investigation of rhodamine (R6G)-doped waveguides and coated optical fibers, the second harmonic light (532 nm) from a Q-switched Nd:YAG laser (10 Hz, ~10 ns pulse width) was incident on the samples at 90° after passing neutral density filters, a variable slit and a cylindrical lens. Typical pumping areas were 0.2 × 1 mm. Emission was detected in an angle of 90° with respect to the exciting light. In all cases, the light emitted from the samples was focused by two lenses on the entrance slit of a 0.25 m monochromator and detected with a liquid nitrogen cooled CCD.

For the detection of photochromism, the UV lines (355/361 nm) of an Ar⁺ ion laser were used for excitation and the transient absorption spectra were recorded by a tungsten lamp. The setup is described in detail elsewhere [16]. Absorption spectra were also recorded in transmission mode on a Shimadzu UV-1610 spectrophotometer.

Secondary electron microscopy (SEM) was performed on a JEOL 6300-F after sputtering the samples with gold. Transmission electron microscopy images were obtained on a JEOL 2000 FX after calcination of the samples at 400°C for 4 h.

3. Results and discussion

3.1. Low-*k* dielectric materials

Dielectric materials with a low dielectric constant *k* (preferentially < 2) are currently in demand for future integrated circuits. SiO₂ (*k* ~ 3.8) is one of the materials investigated in this direction; however, as features are becoming smaller materials with lower dielectric constant are needed (*k* < 2). Possible approaches are the modification of the silicates, e.g. by fluorine doping [17,18]. Another method is to introduce ‘holes’ into the SiO₂ dielectric layer. That can be done, for example, by processing thin films in the presence of dendrimers and calcination of the com-

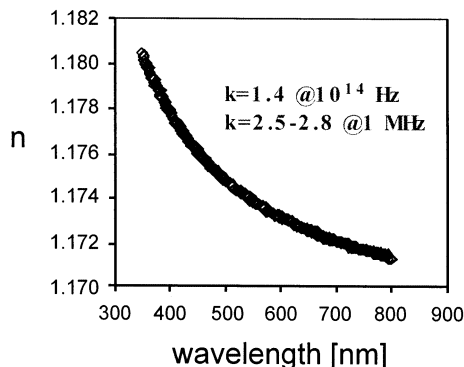


Fig. 2. Refractive index versus wavelength for a mesoporous thin film with p6mm symmetry (thickness = 500 nm).

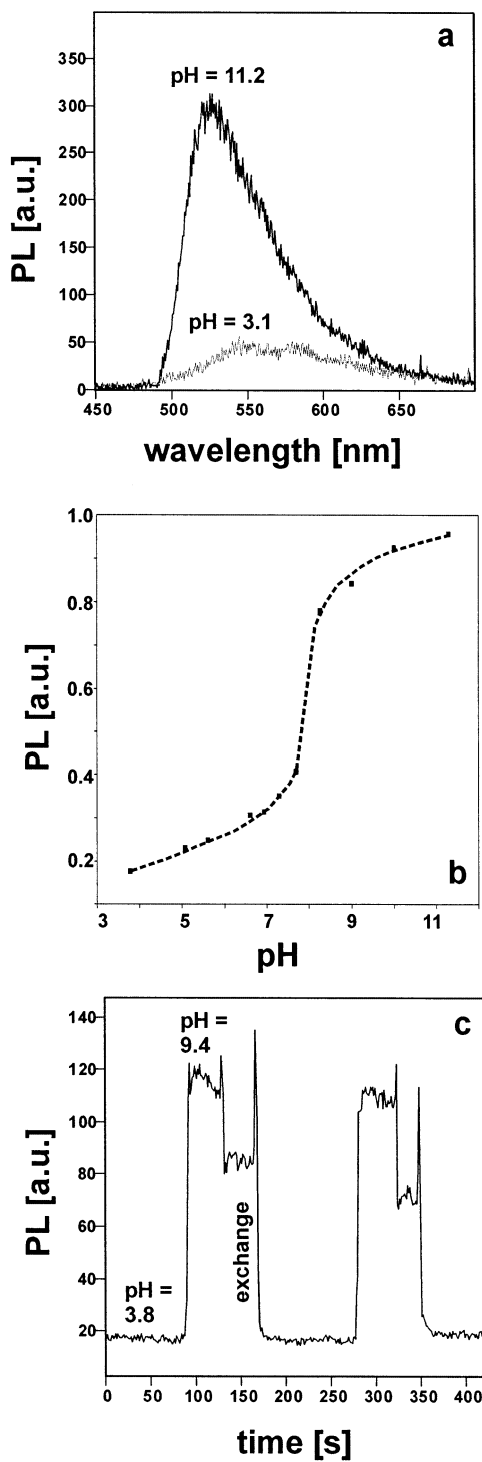
posite material afterwards. Similarly, aerosols have been investigated with respect to their application as low- k dielectrics and are promising materials in this respect [19–21].

Another approach is now offered by employing mesoporous materials. After calcination, these materials consist, in a simple picture, of a regular array of air holes surrounded by a ‘SiO₂ skin’. Since the porosity in these materials can be as high as $\sim 80\%$, k should be significantly lower in comparison to pure SiO₂. We observed, however, that the dielectric constants of the film without HMDS or OTS treatment are high (> 8 at 1 MHz), presumably due to the high density of the surface polar hydroxyl groups. In order to render the inner surface hydrophobic, a vapor treatment with HDMS or OTS had to be employed. Through this CVD step the surface of the mesoporous films became highly hydrophobic and the dielectric constants decreased dramatically to 1.5–2.5 depending on the porosity of the thin film. As expected, larger porosities generally give lower k values for the same mesostructures. Clearly, the refractive index of these materials is also very low ($n \sim 1.15$ – 1.3 , depending on the porosity and structure). Fig. 2 depicts a plot of the refractive index n against the wavelength in the visible range. Such low refractive index materials are useful as support layers for optical materials which have themselves a comparably low refractive index (see below for examples).

Besides the low k value itself, other additional criteria such as high temperature stability, good chemical stability, gap-fill capability etc. must be satisfied [22]. A further important requirement is low water absorption in order to keep k low. We found for the materials investigated here, however, that even with the surface functionalization, the measured dielectric constant is still highly dependent on the humidity and the exposing time to air. When samples were stored at ambient conditions (humidity of ~ 50 – 60%), then within a week the dielectric constants usually rose back to ~ 8 . This reflects the strong tendency of moisture absorption with these high surface area silicas and probably also an incomplete surface functionalization. The current goal is hence the reduction of water uptake during long-term exposure to humidity. This may be achieved by a modification of both the inner pore surface and the pore wall itself. Methods to create mixed inorganic/organic walls are now available [23–25] and together with surface modification they may provide very hydrophobic materials with low k .

3.2. Sensor materials

Another application which can make use of the pores are optical thin film sensors. Formerly, sensing based on optical detection has been implemented in sol-gel glasses [26]. Typically, these sensors are operated by measuring the transmission, emission or lifetime of a complex or an organic dye embedded in an SiO₂ matrix. The response is altered through diffusion of the molecule to be sensed into the matrix towards the sensing dye/complex. Two important tasks in developing such a sensor are the occlusion of the dye/complex (physical occlusion versus covalent anchoring) and the diffusion times which are determined by the glass microstructure. Whereas the first point is important to leaching and hence to long term operation, the second point determines the response times. Principally, the requirements of fast response and negligible leaching can be fulfilled advantageously in large-pore mesoporous materials by covalently anchoring a pH sensitive dye during synthesis and low-temperature block-polymer removal afterwards.



Based on this considerations, we have developed an optical thin film pH sensor with a fast response time [27]. The pH sensitive dye fluoresceinisothiocyanate was derivatized with 3-aminopropyltriethoxysilane. This functionalization ensures that the dye is covalently anchored onto (or within) the SiO_2 wall during mesostructure synthesis. After thin film synthesis employing the block copolymer F127, the ~ 900 nm thick films were dried for about 10 days at room temperature and finally at 70°C for 3–5 days. This prolonged drying treatment is necessary in order to achieve a sufficiently high robustness of the thin films before block-copolymer extraction by ethanol at 80°C . Otherwise, the films exhibit severe cracking after extraction which limits their use in optical sensing devices.

The sensor operates by recording the emission of the anchored dye. In Fig. 3a, a typical plot of the emission spectra upon bringing the thin film into contact with solutions of different pH values is given. Very similarly to what is observed for fluorescein in solution, the integrated emission increases with increasing pH. A typical plot of the emission versus the pH (Fig. 3b) clearly demonstrates that the thin film sensors act analogously to the dye in solution, except that the $\text{p}K_{\text{a}}$ value is shifted from 6.4 in solution to ~ 7.3 in the thin films. In comparison to solution, a broadening of the titration curve is evident. This is attributed to two factors: First, an inhomogeneous dye environment may contribute to this broadening. Second, fluorescein possesses three $\text{p}K_{\text{a}}$ values ($\text{p}K_{\text{a},1} = 2.08$, $\text{p}K_{\text{a},2} = 4.31$, $\text{p}K_{\text{a},3} = 6.43$) which are often difficult to distinguish even in solution [28].

The response time of the thin films is on the order of ~ 7 s for a 95% change in the emission intensity (see Fig. 3c for a typical example). In sol-gel glasses, the response times are much slower than this value, the only exception being small capillaries coated with sol-gel glasses [29]. We conclude that the fast response time is due to the

Fig. 3. pH sensing with a fluorescein-doped, mesoporous thin film. (a) Photoluminescence spectra at pH 3.1 and pH 11.2; (b) Titration curve; (c) Change of photoluminescence upon exchange of pH buffer solutions, demonstrating immediate response of the thin films.

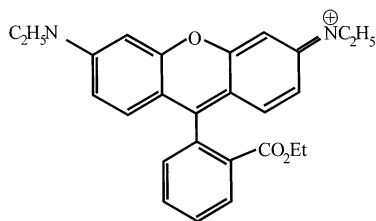


Fig. 4. Structure of rhodamine 6G.

high porosity of the dye carrying mesoporous thin film, since the open pores enable a fast diffusion of the solution towards the dye molecules. This application clearly demonstrates that these mesoporous, highly ordered and transparent thin films of high mechanical robustness are well-suited materials for fast response optical sensors. Future applications in this area also might use patterning methods like inkjet and micro-pen printing of mesostructures in order to generate optical multi-sensor arrays [30].

3.3. Laser materials

Both applications discussed above are based on the porous structure of the calcined or ethanol extracted thin films. It is, however, also possible to use the mesostructure architecture to construct new optical materials with high fidelity by one-step silica/block-copolymer/dye co-assembly. We have explored this by processing mesostructured thin films, waveguides as well as thin films on optical fibers and simultaneously doping these materials with rhodamine 6G, a well-investigated laser dye of the xanthene family. Its structure is depicted in Fig. 4. We choose this dye, because its monomer-dimer(-trimer) equilibrium was investigated for both solutions and when imbedded in sol-gel glasses [31]. For the latter materials it was demonstrated that the spectroscopic properties of the dye are related to the microenvironment it experiences within the sol-gel matrix. Hence, by elucidating the spectral properties of this dye in mesostructured hosts, we can draw conclusions about the dimerization and about the local microenvironment of the dye. We first start with the application of these materials as lasers and compare their properties to that of sol-gel based glasses. We then address the

question, why mesostructured materials have an improved optical performance.

In order to achieve lasing, the mesostructured materials have to be patterned into the appropriate shape. One way is to pattern waveguiding structures by soft lithography [32]. This results in high quality mesostructured line patterns which can be produced within hours (3–12 h). Interestingly, when P123 is used as a block-copolymer, the channels of the p6mm mesostructure are preferentially aligned parallel to the substrate and also along the direction of the waveguides [33]. When these waveguides are optically pumped with the second harmonic light from a Nd:YAG laser (532 nm, 10 Hz), they exhibit amplified spontaneous emission (ASE) [14]. In this process, spontaneously emitted light is amplified by stimulated emission as it propagates along the waveguides. Above a critical pumping energy, this results in a gain-narrowing and super-linear output behavior. The final full-width-at-half-maximum (fwhm) is 7–8 nm, as compared to ~ 60 nm of the photoluminescence spectra well below the threshold (Fig. 5). Since this process does not provide any feedback, the light emitted at the end of the waveguides is usually not spatially and temporally coherent [34]. Despite this, this process is one of several which have been assigned the term ‘mirrorless lasing’ [35]. The threshold for ASE in these waveguides depends on the dye concentration and can be as low as ~ 6 –8 kW cm⁻² at a dye concentration of 1.5 wt.%. In contrast, the threshold for sol-gel glasses having the same dye content, but prepared without block-copolymer is more than an order of magnitude higher (> 200 kW cm⁻²). We attribute this significant difference to the ability of the mesostructure to highly disperse and isolate individual R6G molecules. This lowers the amount of dimers in the final solid which is favorable for obtaining a low-threshold laser material (R6G dimers have low quantum yields).

Feedback for proper lasing can be introduced by fabricating a resonator structure, for example by coating the ends of the waveguides with a metal. We, however, decided to implement another kind of resonator structure which provides feedback and which might also be of importance for direct use in optical devices. Using the μ ring laser design [36], we coated optical fibers (40–125 μ m diameter) first

with a mesoporous thin film by dip-coating followed by calcination. Similarly to the multilayer waveguiding structure, the thin mesoporous film here acts as a low refractive index support. In a further step, the lasing layer is then dip-coated on this support [15]. Now, when optically pumped a fraction of the emitted light is confined to the

outer layer and travels around the μ ring. At a certain threshold of the pumping energy, the gain becomes greater than the loss and lasing is observed at the frequencies given by the condition: $\Delta v = c/d\pi n_{\text{eff}}(n_{\text{eff}} \sim n \sim 1.43)$. A detailed analysis of the waveguided modes shows that they are further modulated by so-called whispering gallery

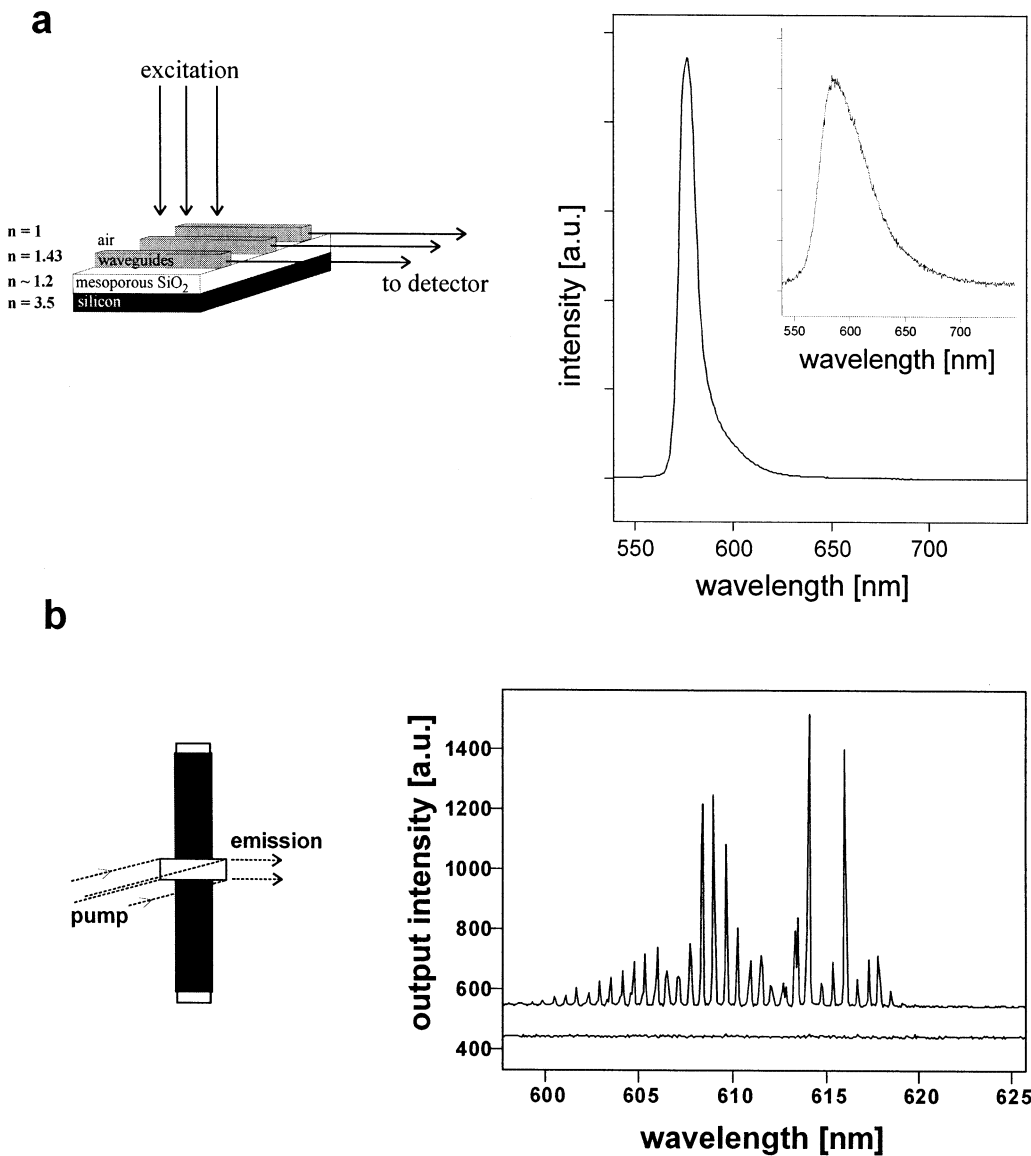


Fig. 5. (a) Amplified spontaneous emission in rhodamine 6G-doped mesostructured waveguides and (b) lasing in rhodamine 6G-doped μ ring lasers. The pictures on the left depict the macroscopic structures and the pumping geometry, the spectra on the right show the emission below and above the threshold.

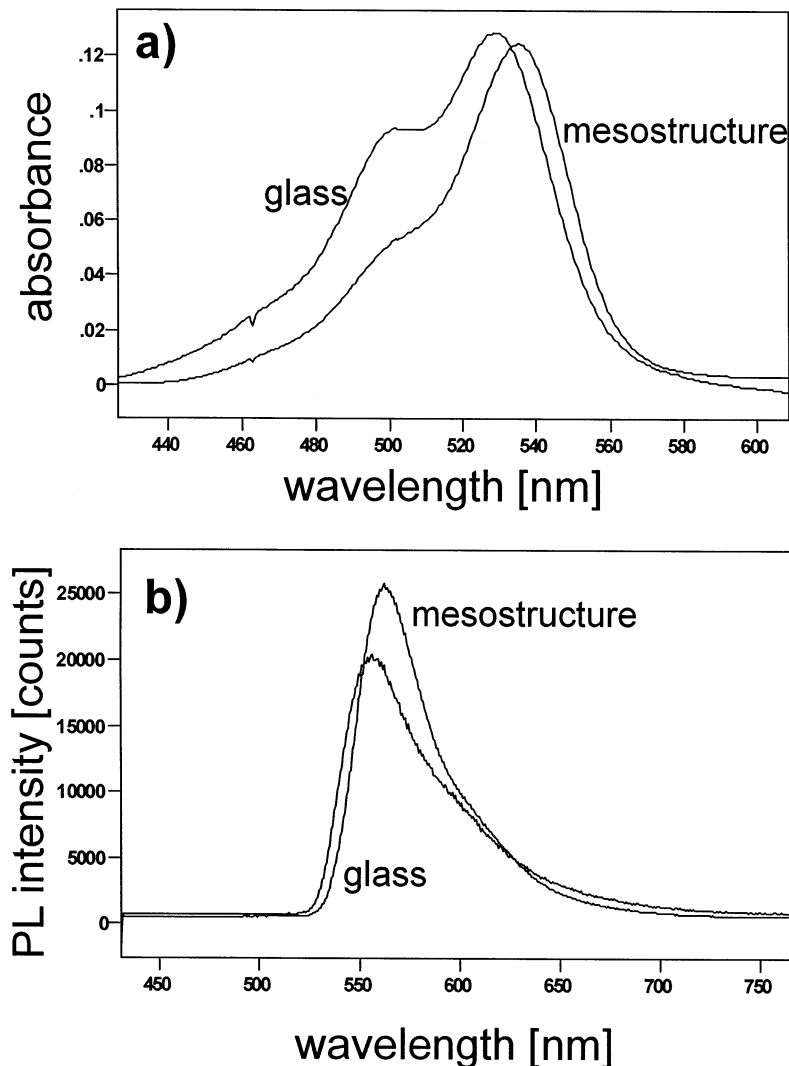


Fig. 6. (a) Absorption spectra of rhodamine 6G occluded in a mesostructured block-copolymer/silica composites and in a sol-gel glass (0.5 wt.%) and (b) corresponding emission spectra. Note that due to the lower quantum efficiency, the emission spectrum of the dye-doped sol-gel glass was multiplied for easier comparison.

modes, which are modes travelling near the outer surface of the dye-doped layer and do not reach the mesoporous film/mesostructured film interface. The threshold for lasing in this μ ring configuration can be as low as $\sim 0.4 \text{ kW cm}^{-2}$ on a $40 \mu\text{m}$ fiber. We note that these values of $\sim 0.4 \text{ kW cm}^{-2}$ compare well with semiconducting polymers ($\sim 0.1\text{--}0.5 \text{ kW cm}^{-2}$ for the best compounds). Furthermore, using smaller fibers

and achieving single mode operation can be expected to further reduce the threshold [37].

We now turn to the question why mesostructured silica/block-copolymer composites are very well suited for lasing applications. In order to get an insight, we analyzed both the UV/Vis absorption and emission spectra as well as the quantum yields of R6G-doped thin films and made a direct comparison to R6G-doped sol-gel glasses. Fig. 6

depicts typical transmission and emission spectra for R6G occluded in p6mm mesostructured thin films and occluded in pure SiO₂ thin films. The dye concentration in the solids is the same for both samples (0.5 wt.%). Several features are evident from the spectra: In the absorption spectra, two absorption bands are clearly distinguished. The first peaks at 530 nm for R6G occluded in sol-gel silica, whereas this peak is shifted to about 536 nm in the mesostructured host (Fig. 6). This red-shift is also observed in the corresponding emission spectra. We attribute this wavelength shift to a change in the microenvironment due to the additional presence of the block-copolymer which interacts with the dye molecules. Moreover, absorption spectra reveal that the dimer band at about 502 nm in the case of the sol-gel glass (507 nm for the mesostructured host) is much more pronounced in the former case. Hence, dimerization of the dye molecules is considerably reduced in mesostructured materials. An explanation for this finding is that the dye molecules co-assemble within the hydrophobic domain of the block-copolymers or are occluded in the PEO domain, respectively. The block-copolymer–dye interaction leads to a high dispersion of the occluded dyes since the probability for dye–dye interaction is reduced. Since it is known that R6G dimers have much lower quantum efficiencies than monomers, this also explains and underlines the superior lasing properties for R6G-doped mesostructured materials. This is further supported by quantum efficiency measurements which quantitatively demonstrate that dimerization for R6G is largely reduced in block-copolymer/silica nanocomposites in comparison to pure sol-gel SiO₂ glasses. A systematic investigation for R6G concentrations from 0.1 to 2.5 wt.% shows that with increasing dye concentration, the quantum efficiencies decrease. However, for all concentrations investigated, the quantum efficiencies of the mesostructured materials are significantly higher (by at least about one order of magnitude) than those of the dye-doped sol-gel glasses [38]. This finding clearly underlines the conclusion from the UV/Vis absorption spectra that the R6G dye molecules are much better isolated within these organic/inorganic nanocomposites. The

higher quantum efficiencies also explain the significantly lower thresholds for lasing in these novel systems.

3.4. Photochromic materials

Mesostructured materials can also host photochromic dyes, i.e. dyes which change their color upon light illumination [39]. For spiropyrane and spirooxazine derivatives, this is due to ring opening of the molecules upon light action going hand in hand with a color change. For applications, it is desirable that the reverse reaction (thermal bleaching) is fast, which allows rapid switching between two states (high/low transmission in a certain wavelength range). Inorganic, organic and mixed inorganic/organic have been investigated as matrices. For purely inorganic host materials, the response times are slow in comparison to solution (minutes versus seconds) and undesired reverse photochromism is often observed in these matrices [40–42]. In organic matrices, on the other hand, the response can be much faster (in the order of seconds) [43]. However, these pure organic materials like PMMA possess lower thermal stability and mechanical robustness than glasses. Besides, in these matrices more than one site is available for the dye which then results in a multiple distribution of response times. The properties can be improved, however, by blending inorganic and organic components on a molecular level. A bleaching constant of 0.2 s⁻¹ was reported for a spirooxazine molecule embedded in an organically modified silicate [44], which is as fast as the response time of the same dye in ethanol solution.

In this context, we explored mesostructured block-copolymer/silica composites, since a priori we expected these matrices to be excellent hosts to provide the materials base for the requirements discussed above. Thin films were prepared by dip-coating dye-doped precursor solutions. When doped with 1,3-dihydro-1,3,3-trimethylspiro[2*H*-indole-2,3'-[3*H*]naphth[2,1-*b*][1,4]oxazine], a spirooxazine derivative, the thin films are colorless and exhibit a transmission ~100% throughout the visible spectrum. However, when the thin films are illuminated with 355 nm light from an

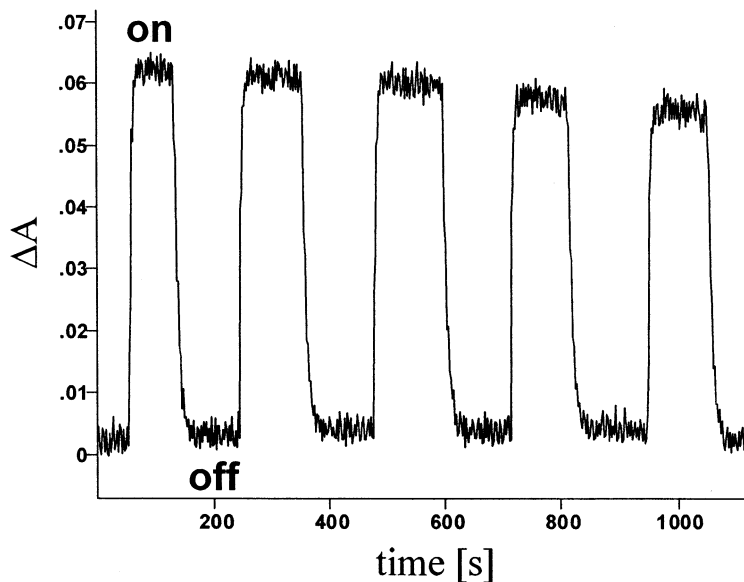


Fig. 7. Change in absorbance of photochromic mesostructured thin films doped with a spirooxazine during several light on/off cycles.

UV lamp, they become immediately blue. Upon removal of the light source, they become completely colorless again, the entire thermal back-fading process taking only a few seconds. The change in absorbance during several light on/off cycles is depicted in Fig. 7.

A detailed analysis of the bleaching kinetics revealed a rate constant for back-fading $k = 0.15 \text{ s}^{-1}$ which compares well to the best value reported for this molecule in a solid matrix so far. The bleaching curves can be fitted by mono-exponential functions indicating a homogeneous dye environment. Based on the fact that the dye exhibits only normal photochromism, we conclude that the dye is located within the organic part of the composite, most probably within the PEO sub-domain. This is supported by the fact that in sol-gel glasses prepared without block-copolymers the same dye shows (i) a much slower response; and (ii) begins to exhibit reverse photochromism (compounds are colored in the dark and become colorless upon light illumination) after prolonged aging. This is attributed to a stabilization of the open form by the silica host through hydrogen bonding. Here, it is interesting to note that the rate constant for back-fading of the spirooxazine increases with

prolonged consolidation time of the thin films. Whereas $k = 0.09 \text{ s}^{-1}$ for fresh films (2 days old), k increases to 0.15 s^{-1} for 3 weeks old films. This demonstrates that hydrolysis/condensation is ongoing during this aging process. As a consequence, the amount hydroxyl-groups on the silica surface reduces, hence providing less hydrogen binding sites for the open form of the dye.

We conclude that by direct doping of mesostructured silica/block-copolymer composites with spirooxazine and spiropyran molecules, the latter predominantly co-assemble with the block-copolymer and are finally located within the organic part of the composite. This makes these materials different from purely inorganic SiO_2 sol-gel glasses as evidenced by the different spectral properties of the occluded dyes and demonstrates that a more sophisticated microenvironment tuning is offered by mesostructured materials.

4. Conclusions

Mesoporous and mesostructured materials derived by a combination of block-copolymer templating and weakly acidic sol-gel chemistry are

attractive candidates for low- k materials and optical applications such as lasers, optical sensors, and photochromic materials. Under weakly acidic conditions, they can be processed similarly to sol-gel glasses, allowing one to bring them into a desired macroscopic shape. The main differences compared to sol-gel glasses are, however, the ordered sequence of either holes/silica or block-copolymers/silica on the nanometer scale. The high porosity of calcined, mesoporous materials offers new possibilities for low- k materials engineering. After proper inner surface treatment, their dielectric constants are comparably low ($k \sim 2$) and are in the range required for future-generation integrated circuits. As the pores are also accessible by vapors and liquids, they are an excellent starting point for new optical sensor components. The sensing of the pH of solutions is a first example; however other sensing applications in the fields vapor composition, O₂ content in water etc. might be envisioned. Moreover, we expect the combination of the sensing capabilities together with fast processing techniques and pattern recognition to lead to optics based multiple-sensor arrays which can evaluate the composition of vapors and liquids in the microsecond domain.

Mesostructured materials are very efficient for dye doping. Dyes can be incorporated in high concentrations by still having isolated dye molecules in the final solids, a property which is useful in creating low-threshold laser materials and fast-response photochromic composites with a high change in absorption. Moreover, the block-copolymers are determining the local molecular environment of the occluded dyes. The latter property might also be useful for constructing more complex composite materials which are currently under investigation. For example, one could envision an energy-transfer system, in that, that the block-copolymer (or surfactant) carries an optically active unit which transfers energy to a nearby located dye after excitation.

Acknowledgements

We thank V.I. Srdanov and M.D. McGehee for fruitful discussions and assistance during this

work. The work presented here was supported by the NSF under grant DMR-95-20971 and the U.S. Army Research Office under grant DAAH04-96-1-0443. It made use of the Materials Research central facilities supported by the NSF under award DMR-9632716. G.W. acknowledges support from the Austrian Science Foundation for an Erwin-Schrödinger-fellowship (J1643-CHE).

References

- [1] Q. Huo, D.I. Margolese, U. Ciesla, P. Feng, T.E. Gier, P. Sieger, R. Leon, P.M. Petroff, F. Schüth, G.D. Stucky, *Nature* 368 (1994) 317.
- [2] D. Zhao, J. Feng, Q. Huo, N. Melosh, G.H. Fredrickson, B.F. Chmelka, G.D. Stucky, *Science* 279 (1998) 548.
- [3] D. Zhao, Q. Huo, J. Feng, B.F. Chmelka, G.D. Stucky, *J. Am. Chem. Soc.* 120 (1998) 6204.
- [4] B.C. Bunker, P.C. Rieke, B.J. Tarasevich, A.A. Campell, G.E. Fryxell, G.L. Graff, L. Song, J. Liu, J.W. Virden, G.L. McVay, *Science* 264 (1994) 48.
- [5] A. Sayari, *Chem. Mater.* 8 (1996) 1840.
- [6] A. Corma, *Chem. Rev.* 97 (1997) 2373.
- [7] D. Zhao, P. Yang, N. Melosh, J. Feng, B.F. Chmelka, G.D. Stucky, *Adv. Mater.* 10 (1998) 1380.
- [8] S. Baskaran, J. Liu, K. Domansky, N. Kohler, X. Li, C. Coyle, G.E. Fryxell, S. Thevuthasan, R.E. Williford, *Adv. Mater.* 12 (2000) 291.
- [9] G. Wirnsberger, G.D. Stucky, *Chem. Eur. J. Chem. Phys.* 1 (2000) 90.
- [10] H.S. Zhou, I. Honma, *Adv. Mater.* 11 (1999) 683.
- [11] D. Avnir, D. Levy, R. Reisfeld, *J. Phys. Chem.* 88 (1984) 5956.
- [12] N.A. Melosh, P. Lipic, F.S. Bates, F. Wudl, G.D. Stucky, G.H. Fredrickson, B.F. Chmelka, *Macromolecules* 32 (1999) 4332.
- [13] Pluronic is a registered trademark of BASF cooperation.
- [14] P. Yang, G. Wirnsberger, H.C. Huang, S.R. Cordero, B. Scott, M.D. McGehee, T. Deng, G.M. Whitesides, B.F. Chmelka, S.K. Buratto, G.D. Stucky, *Science* 287 (2000) 465.
- [15] G. Wirnsberger, G.D. Stucky, *Chem. Mater.* 12 (2000) 2525.
- [16] G. Wirnsberger, B.J. Scott, B.F. Chmelka, G.D. Stucky, *Adv. Mater.* 12 (2000) 1450.
- [17] S.W. Lim, Y. Shimogaki, Y. Nakano, K. Tada, H. Komiyama, *Jpn. J. Appl. Phys.* 35 (1996) 1468.
- [18] K. Kim, D.H. Kwon, G. Nallapati, G.S. Lee, *J. Vac. Sci. Technol. A.* 16 (1998) 1509.
- [19] D.M. Smith, D. Stein, J.M. Anderson, W. Ackerman, *J. Non-Cryst. Solids.* 186 (1995) 104.
- [20] L.W. Hrubesh, L.E. Keene, V.R. Latorre, *J. Mater. Res.* 8 (1993) 1736.

- [21] M.-H. Jo, J.-K. Hong, H.-H. Park, J.-J. Kim, S.-H. Hyun, *Microelectr. Eng.* 33 (1997) 343.
- [22] H. Treichel, G. Ruhl, P. Ansmann, R. Würfl, C. Müller, M. Dietlmeier, *Microelectr. Eng.* 40 (1998) 1.
- [23] B.J. Melde, B.T. Holland, C.F. Blanford, A. Stein, *Chem. Mater.* 11 (1999) 3302.
- [24] S. Inagaki, S. Guan, Y. Fukushima, T. Ohsuna, O. Terasaki, *J. Am. Chem. Soc.* 121 (1999) 9611.
- [25] T. Asefa, M.J. MacLachan, N. Coombs, G.A. Ozin, *Nature* 402 (1999) 867.
- [26] R. Zusman, C. Rottman, M. Ottolenghi, D. Avnir, *J. Non-Cryst. Solids.* 122 (1990) 107.
- [27] G. Wirnsberger, B.J. Scott, G.D. Stucky, *Chem. Commun.* 2001, 119.
- [28] R. Sjöbäck, J. Nygren, M. Kubista, *Spectrochim. Acta. A.* 51 (1995) L7.
- [29] J. Samuel, A. Strinkovski, S. Shalom, K. Lieberman, M. Ottolenghi, D. Avnir, A. Lewis, *Mater. Lett.* 21 (1994) 431.
- [30] H. Fan, Y. Lu, A. Stump, S.T. Reed, T. Baer, R. Schunk, V. Perez-Luna, G.P. López, C.J. Brinker, *Nature* 405 (2000) 56.
- [31] U. Narang, F.V. Bright, P.N. Prasad, *Appl. Spectrosc.* 47 (1993) 229.
- [32] Y. Xia, G.M. Whitesides, *Ann. Rev. Mater. Sci.* 28 (1998) 153.
- [33] G. Wirnsberger, P. Yang, H.C. Huang, B.J. Scott, T. Deng, G.M. Whitesides, B.F. Chmelka, G.D. Stucky, *J. Phys. Chem. B.*, in press.
- [34] W.T. Silfvast, *Laser Fundamentals*, Cambridge University Press, Cambridge, 1996.
- [35] A.E. Siegman, *Lasers*, University Science Books, Mill Valley 1986.
- [36] H.P. Weber, R. Ulrich, *App. Phys. Lett.* 19 (1971) 38.
- [37] M. Kuwata-Gonokami, R.H. Jordan, A. Dodabalapur, H.E. Katz, M.L. Schilling, R.E. Slusher, *Opt. Lett.* 20 (1995) 2093.
- [38] G. Wirnsberger, P. Miranda, J. Schmitt, S.K. Buratto, B.F. Chmelka, G.D. Stucky, in preparation.
- [39] G.H. Brown (Ed.), *Photochromism, Techniques of Chemistry*, vol. III, Wiley-Interscience, New York, 1971.
- [40] V.R. Kaufman, D. Levy, D. Avnir, *J. Non-Cryst. Solids.* 82 (1986) 103.
- [41] D. Levy, D. Avnir, *J. Phys. Chem.* 92 (1988) 4734.
- [42] D. Preston, J.-C. Pouxviel, T. Novinson, W.C. Kaska, B. Dunn, J.I. Zink, *J. Phys. Chem.* 94 (1990) 4167.
- [43] M. Levitus, P.F. Aramendia, *J. Phys. Chem. B.* 103 (1999) 1864.
- [44] B. Schaudel, C. Guermeur, C. Sanchez, K. Nakatani, J.A. Delaire, *J. Mater. Chem.* 7 (1997) 61.